Local order structure of lead borate glasses doped with Sm_2O_3 correlated with IR study

A. ABOU SHAMA*, M. BAHAA EL-DEN, YASSER A. EL-GAMMAM
Ain Shams University, Faculty of Science, Physics Department 11566 Abbassia, Cairo, Egypt

The local order structure was studied for the amorphous $0.7PbO\text{-}0.25B_2O_3\text{-}0.05Al_2O_3$ glasses doped with 0.5, 2.0 and 5.0 gm of Sm_2O_3. The radial distribution analysis for both short range order (SRO) and medium range order structure (MRO) was applied for the collected XRD data. The sine Fourier transform was performed on the extracted interference function in the inverted space to get on the inter-atomic pair distribution function in the real space. The role of Sm_2O_3 introduced in the matrix was found to modify the atomic correlated distances of the detected atomic pairs and also their coordination numbers. This role of Sm_2O_3 was highly observed in the samples 3 and 4 containing 2.0 and 5.0 gm of Sm_2O_3 to change AlO_4 and BO_3 to AlO_6 and BO_4 forms. Three evidenced main peaks were observed at the ranges (2.33-2.54)Å, (4-4.16)Å and (6.65-6.74)Å respectively with the un-doped and doped samples with Sm_2O_3. These observed peaks were belonging to Pb-O, Pb-Pb in the SRO and Pb-O of the second order in the MRO. The assigned pairs were arranged in the form PbO_3 units while the metallic Pb-Pb pairs were of tetrahedral units. The second and successive RDF peaks are of composite structure (can be resolved into more than one atomic pair); accordingly, a small unresolved pre and post shoulders may be predicted in SRO and MRO regions which belonging to B-O and Sm-O correlated pairs. The other correlated pairs such as, Al-Al and Sm-Sm were not evidenced due to their small introduced weights in the given amorphous matrix. The extracted structural information's were correlated with the measured IR for these studied samples and the IR studies gave a good consistency with the RDF analysis for the detected atomic pairs.

(Received December 19, 2011; accepted February 20, 2012)

Keywords: SRO, MRO, Tetrahedral units, Inter-atomic correlations, Network units and IR correlation

1. Introduction

Rare-earth (RE) ion-doped glasses have been paid much attention because of their high potential use for optical applications such as fibers, amplifiers, lasers and sensors. The primary objective of this strategy involves determining the glass composition that can homogeneously dissolve large amounts of RE oxides (Re_2O_3). Among the glass components, Al_2O_3 has received significant consideration as the most likely matrix composition due to its high solubility of rare-earth ions [1,2]. Re_2O_3 has a structure similar to that of Al_2O_3 in which the RE ions have a preference for eight-fold or nine fold coordination. The charge of RE ions is compensated by the oxygen's surrounding the Al^{3+} ions, which results in a homogeneous dispersion of the RE ions in the glass structure. However, in the meantime, it is difficult to prepare a glass containing large amounts of Al_2O_3 because of its high melting temperature.

In recent years, considerable attention has been devoted to the search for new materials to be used as hosts for RE ion impurities. These ions can be incorporated easily into several glass matrices, which can make them suitable to achieve laser radiation due to the appearance of sharp and unambiguous absorption bands in their optical transmission spectra [3].

Glasses doped with RE atoms are well known as fluorescent substances because of their high luminescence efficiency. Glasses containing various RE ions are seen as promising materials for quantum electronics devices such as high power lasers [4-7]. Trivalent samarium ion has been used as an active ion in various glass and crystal hosts. Sm^{3+} ions yield strong emissions in visible region, leading to lasing, both in compact fiber and planar geometries [8]. Recently, in particular Sm^{2+} doped materials are of great importance with non-linear optical hole burning which leads to using it as an optical data storage materials [9-11]. Preparation of Sm^{2+}-doped glasses requires carefully optimized melting conditions due to the instability of the divalent state of samarium. Neverthless, the reduction process of Sm^{3+} has attracted relatively little attention in literature. Equilibrium of the redox reaction responsible for reduction of Sm^{3+} to Sm^{2+} depends on the partial pressure of oxygen in the melting furnace, composition of the glass, crucible material, melting temperature, cooling rate, etc. The role of Al_2O_3 in the reduction of samarium in silicate glasses has been discussed by Nogami et al. in 1998 [12, 13].

The main task of this work is to investigate the structure of $0.7PbO\text{-}0.25B_2O_3\text{-}0.05Al_2O_3\text{-}xSm_2O_3$ glasses (x=0.0, 0.5, 2.0 and 5.0 gm) using XRD data Fourierly transformed to obtain radial distribution function (RDF), real space information's in both SRO and MRO, giving an evidence to the role of Sm_2O_3 introduced in the studied amorphous matrix and correlate them with IR study for these specimens.

2. Experimental work

A. Preparation of the glass specimens

Glass system of $0.7PbO\text{-}0.25B_2O_3\text{-}0.05Al_2O_3$ with varing doping amounts of samarium oxide ranging from 0.0 to 5.0 gm are prepared by mixing appropriate weights of raw materials, H_3BO_3, Pb_3O_4 and Al_2O_3 of grade purity in porcelain crucibles. The mixture is heated in an electric furnace at 1223 K. Synthesis process is continued for 2 hours to ensure complete homogeneity .Then, the melt is poured and preheated onto circular stainless steel mold of radius 1.3 cm and the samples are annealed at temperature 673 K to avoid and minimize the stress-strain in the fresh samples.

B. Hydrostatic density measurements

The densities of the prepared glass samples were measured in an indirect method based on Archimedes' principle using xylene as immersion liquid according to the equation:

$$\rho = \frac{wt_a}{wt_a - wt_{lq}} \times \rho_{lq} \quad g/cm^3$$

Where:

1. ρ is the required glass sample density.
2. wt_a the weight of the glass sample in air.
3. wt_{lq} the weight of the glass sample in the immersing liquid.
4. ρ_{lq} the density of the immersing liquid.

The composition and the density of the glass samples used in investigated optical and structural properties are shown in Table 1.

Table 1. Composition and density of the glass batches.

Glass no.	Composition %			gram (per batch)	Density g/cm^3
	B_2O_3	PbO	Al_2O_3	Sm_2O_3	
(1)	25	70	5	0.0	5.143
(2)	25	70	5	0.5	5.025
(3)	25	70	5	2.0	5.131
(4)	25	70	5	4.0	5.291

C. XRD apparatus setup

The present data were collected by using Philips (X'pert MPD) diffractometer using the Bragg-Brentano para-focusing technique. Highly monochromated Cu-radiation (wavelength λ= 1.54051Å) was used. The step scan mode was applied in the 2θ-range (4-157.4612°). The step size ($\Delta 2\theta$= 0.04°) and the counting time was 10 sec. for each reading. The corresponding accessible maximum scattering vector magnitude, K, was 8.0 Å^{-1}. The air scattering was avoided by a suitable applied arrangement of XRD system. The receiving and divergence slits were properly chosen in both small and large 2θ-ranges, in order to improve the qualities of data collected as it could as it possible.

D. IR absorption measurements

Fourier transform infrared (FTIR) absorption spectra of the studied glasses are measured in the range 4000-500 cm^{-1}, using the KBr-pellet method at room temperature. A recording spectrophotometer type, Jasco V-570 UV/VIS/NIR (Japan), is used.

3. Results and discussion

The scattered intensity in the K-space is corrected for the polarization and absorption, scaled and normalized to get on the self scattered intensity and the structure factor S(K) [14-16].

Fig. 1 depicts the structure factor of the investigated amorphous matrix, free and doped with 0.5, 2.0 and 5.0 gm of Sm_2O_3, in the reciprocal space (K-space; $K=4\pi\sin\theta/\lambda$, λ=1.54051Å and K_{max}=8.0Å^{-1}) using the cupper radiation source. A pre-shoulder to the first scattering peak is observed at 1.32Å^{-1} for all the set of samples. This shoulder is related to the structure of the MRO arranged atomic pairs [17, 18] and it may be related to the B-O atomic pairs in the SRO due to its correct position in belonging to these atomic correlations having nominally small weights in the amorphous matrix. Also, it is clear that this shoulder location is independent of the introduced Sm_2O_3 component in the prepared lead- borate-aluminate samples. The next more sharper peak which belongs to SRO structure is evidenced at ~2.00Å^{-1} for all the investigated samples. The third assigned scattering peak is of composite structure and is located at about 3.253Å^{-1} with a broadening 3.0-3.481Å^{-1} with a post shoulder at 3.651Å^{-1} and the second sample had this third K at 3.2310Å^{-1} with the same previous broadening as in sample one but, with a post shoulder at 3.6720Å^{-1}. The last two samples (doped with 2.0 and 5.0 gm of Sm_2O_3) had the first K with its pre-shoulder as in the previous two samples; at 1.32 and 2.0Å^{-1} respectively. The next higher K-space peaks for sample three are located at: (3.19-4.07), 4.53, (4.88-5.67), 5.86 and (6.52-7.61)Å^{-1} respectively. The sample four has a more extent K's; for K_2 which is assigned at ~ 3.314-4.24Å^{-1} with the next higher K locations at 4.956-5.6Å^{-1}, 6.4-6.8Å^{-1} and finally K_5 at

7.641Å^{-1}**.** The previous K-ranges for the investigated samples are given in Table 2. The observed K_{max} to ~ 8.0Å^{-1} will only give the ability of RDF analysis to be limited to the MRO extracted information's without extended data resolution**,** taking in mind the less availability of XRD normal sources signal to noise ratio compared with data collected of storage rings producing synchrotron beams.

Fig. 2 shows the "Radial Distribution Function", RDF (Atoms/Å), versus the radial distance r (Å) for amorphous $0.7PbO\text{-}0.25B_2O_3\text{-}0.05Al_2O_3$ doped with 0.0, 0.5, 2.0 and 5.0 gm respectively of Sm_2O_3. The first ordered shell is belonging to Pb-O correlated pairs and is centered at 2.313Å for the first un-doped sample, shifted to 2.421Å in the second one and is shifted to ~2.541Å in the last two samples (doped with 2.0 and 5.0 gm of Sm_2O_3). This shell is highly disordered having an area of ~2.511 atoms which means that P-O pairs are arranged in the form PO_3 triangles form. It is clear that the doping of Sm_2O_3 in the amorphous matrix changes only the bond distance correlation of Pb-O by about 0.32Å without changing its arranged form of triangles. The second observed RDF peak for un-doped sample is evidenced at 4.11Å having a coordination number of 4.0 which is belonging to Pb-Pb atomic correlations. This peak for the first sample having a pre-shoulder at 3.30Å which is due to B-O correlations formed of BO_3 units and a post shoulder at 4.86Å which attributable to Pb-O correlated second order pairs arranged also in the form PbO_3 in the medium range order (MRO) structure. The next broadened peak is centered at 6.75Å which is belonging to Pb-Pb second order atomic pairs having a coordination number 4.0. This third main peak can be resolved into two preceded peaks at 6.25Å and 6.55Å which are attributed to, may be, Al-O and Pb-O pairs each of which had a tetrahedral form of AlO_4 and PbO_4 respectively. In the second sample (Sm_2O_3=0.5 gm), a shift to a longer distance is observed in the first two peaks to be located at 2.42Å and 4.16Å respectively with nearly the same previous coordination numbers as in sample one, while the third peak is shortened to be at 6.63Å. One can observe an evolution of good Gaussian shape for the second peak; also the absence of pre and post peak shoulders as observed in the first un-doped sample (Sm_2O_3=0.0 gm). The Pb-O correlations are still centered at 2.42Å having the form PbO_3 and the second peak can be analyzed into more than one atomic pair correlation. This second peak as a composite structure peak is formed of BO_3 coordination's at ~3.4Å, Pb-Pb pairs of tetrahedral arrangement at 4.16Å and Sm-O correlations, may be, at ~4.56Å having SmO_3 form. These observations may be an indication to the replacement of Pb-O second order correlations (as noted in sample one) by Sm-O coordinated units. The third observed peak in the second sample which was assigned at 6.63Å is due to Pb-Pb correlations preceded also by AlO_4 units at about 6.10Å and PbO_4 units at ~6.21Å respectively.

In the third sample (Sm_2O_3=2.0 gm), a large structural modifications can be detected due to the introduction of Sm_2O_3 as a modifier component. The first coordination shell is evidenced at a longer distance ~2.552Å and the second main coordination shell is highly shortened to be at around 4.0Å and a good resolved shoulder is observed at ~4.85Å**.** The third ordered shell is elongated again to be at 6.80Å with a pre-shoulder at 6.0Å. The observed changes in the coordinated pairs are in the SRO arranged units, PbO_3 have no, change while BO_3 units changed to BO_4 forms at 3.55Å. In the MRO region, Pb-Pb coordinated atomic pairs had 4.0 coordination number, and SmO_3 building units are predicted at 4.85Å. The third main peak which is stretched to be at 6.80Å (Pb-Pb second order pairs of coordination number 6.0) is preceded by AlO_4 and PbO_4 building units. The tetrahedral units of AlO_4 and PbO_4 are located at 6.0Å and 6.40Å respectively. One can observe from RDF of the third sample containing 2.0 gm of Sm_2O_3, that the introduction of Sm_2O_3 in the matrix will highly manifest the appearance of both Sm-O and Al-O pairs at 4.85Å and 6.00Å respectively and changing the coordination number of metallic Pb-Pb pairs from 4.0 to 6.0 atoms.

In the last sample having Sm_2O_3 content of 5.0 gm, the first coordinated sphere of PbO_3 units is centered as before in sample 3 at ~2.551Å followed by the two main observed peaks at 4.08Å and 6.65Å respectively. One can observe the disappearance again of the pre and post shoulders attached to the second and third peaks as noticed in the previous third sample, instead a broad valley is created between these second and third peaks. This can give an indication to the highly stabilized ordered pairs inside both SRO and MRO regions with the high introduced Sm_2O_3 content. The two main successive long distance peaks may be resolved into more than one contribution as given before. The Sm-O correlations are completely disappeared giving a chance for AlO_4 units to be changed into AlO_6 octahedral units at almost 6.10Å followed by PbO_4 at ~6.40Å and the peak maximum for Pb-Pb of second order correlations are located at 6.65Å smaller by about 0.15Å compared to the previous third sample. The degree of the matrix disorder may increase due to the dissociated Sm-O pairs into separate Sm-ions, in the meantime, increasing of bonded oxygen atoms to the Al-O correlations to be in the form of AlO_6 units.

Despite the increased broadening of RDF peaks in sample 4 a new evolved small peaks may be observed at about 8.05Å and 8.55Å respectively compared to other previous samples which indicates to an increased order beyond the MRO structural region. It should be noted that the good flattening of RDF beyond the first three main peaks in the first two samples compared to the last two samples can be interpreted in terms of two reasons: the first one is the quality of XRD collected data in K-space (as an example, the signal/noise ratio of X-ray applied beams) and the second reason is produced from the role of modifier(s) introduced in the main amorphous matrix as Sm_2O_3 in our investigated samples. The data truncated range in K-space as well as the other implemented parameters are fixed for all samples to perform the Fourier transform and to get on RDF real space information's in both SRO and MRO regions. The extracted information's are highly settled and having a good stability for peak positions, peak areas and peak "Full Width Half

Maximum" (FWHM), (R, N, σ), for all the treated samples.

Unfortunately, the articles published for the RDF analysis for the given prepared samples; 0.7PbO-$0.25B_2O_3$-$0.05Al_2O_3$-xSm_2O_3(x=0.0, 0.5, 2.0 and 5.0 gm) are very rare despite many articles are involved for other physical studies.

4. Bond angle distributions in the investigated samples

The investigated samples of 0.7PbO-$0.25B_2O_3$-$0.05Al_2O_3$-xSm_2O_3(x=0.0, 0.5, 2.0 and 5.0 gm) having the bond linkages in the SRO of Pb-Ô-Pb distribution as: 126.021° for the un-doped sample and this angle decreases with the introduction of Sm_2O_3 as 0.5 gm in the matrix to be 118.304° which means that the contribution of Sm_2O_3 inside this amorphous system relaxes the Pb-Ô-Pb correlations connected in the SRO range. This behavior is highly evidenced in the following samples having larger Sm_2O_3 content (2.0 and 4.0 gm respectively). The last two samples had Pb-Ô-Pb of lower angles as before, 103.93° and 106.864°. As a consequence, the increased Sm_2O_3 content in the given samples increases the relaxation of the lead oxygen correlated bonds despite the extension occurred in Pb-O pairs from 2.323Å to 2.541Å, but this extension in Pb-O bonds is associated with a shortening in Pb-Pb pairs from about 4.16Å to ~4.0Å. Accordingly, the Sm_2O_3 role in the studied samples is well established as a modifier in bond lengths and bond angles in SRO range and changing the bond lengths and bond coordination in MRO in an appreciable weight compared to the degree of angle relaxations. As noted previously, also for the bond linkages Pb-Ô-B the role of introduced Sm_2O_3 in the given amorphous matrix was to relax these bond angles having the values: 90.5168°, 89.2058° and 88.1394° respectively, but for the last sample the presence of B-O in the MRO (3.30-3.55Å) was not revealed. These findings are supporting the previous XRD structural information's reported in the above section.

Table 2. The K-maxima in the reciprocal space, $Å^{-1}$, for the investigated amorphous samples of lead borate aluminate doped with Sm_2O_3.

Sample Number	Sm_2O_3 (gm)	K_1(sh.)	K_2	K_3	K_4	K_5	K_6	K_7	K_8	K_9	K_{10}
1	0.0	1.32	2.0	3.3	4.28	5.04	6.05	6.63	7.16	7.45	_
2	0.5	1.32	2.0	3.3	4.28	5.04	6.05	6.63	7.16	7.45	_
3	2.0	1.32	2.0	3.24	3.95	4.78-5.6	6.6	7.0	7.56	_	_
4	5.0	1.32	2.0	3.28	3.75	4.2	4.96	5.16	5.52	6.36-6.85	7.64

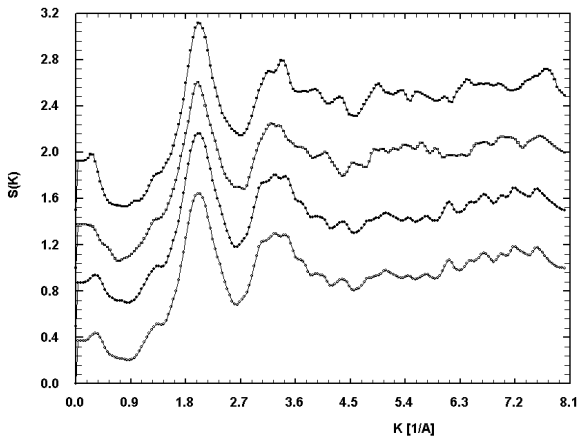

Fig. 1. Total structure factor S(K) versus K for a-0.7PbO-0.25B_2O_3-0.05Al_2O_3-xSm_2O_3; x=0.0, 0.5, 2.0 and 5.0 gm respectively from bottom to top.

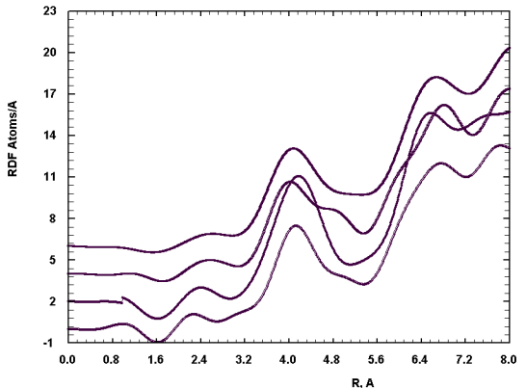

Fig. 2. Total RDF of a-.70PbO-0.25B_2O_3-0.05Al_2O_3 doped with Sm_2O_3 of 0.0 gm, 0.5 gm, 2.0 gm and 5.0 gm respectively from bottom to top.

5. IR studies

The IR spectrum of sample "1" (0.0 gm of Sm_2O_3) shows many bands in the ranges 1100-1500 cm^{-1}, 800-1100 cm^{-1} and ~700 cm^{-1}. The first region is attributed to the asymmetric stretching relaxation of the B-O bond of

triangles BO_3 units, the second is due to the B-O bond stretching of the tetrahedral BO_4 units, and the bond observed around 700 cm^{-1} is due to bending mode of B-O-B linkages in the borate networks. The absence of band at 806 cm^{-1} indicates the absence of boroxol rings [19]. Ultimately, the glass sample consists of BO_3 and BO_4 groups linked randomly.

Actually, the bands due to BO_3 and BO_4 groups apparently take place while suffering shifts toward lower wave numbers where the citations of their locations in literature cover higher values of wave number. The range 950-1085 cm^{-1} was attributed to BO_4 by Upender G. et al. [20], 1023 cm^{-1} by Virender Kunder et al. [21], 990 cm^{-1} by Andelean I. et al. [22] and 1004 cm^{-1} by Motke S.G. et al. [23].

For BO_3 units, bands at 1333-1390 cm^{-1}, Upender G. et al. [20], 1445 cm^{-1},Virender K. et al. [21], 1400 cm^{-1} [23,24], 1420 cm^{-1}, Andelean I. et al. [22], 1357 cm^{-1}, Motke S.G. et al. [23, 24]. The appearance of these bonds in the spectrum of sample "1" at lower wave numbers than generally reputed values can be attributed to the effect of PbO. Lead incorporation into glass matrix does not originate new FTIR bonds, however, it can be concluded that the shift of the vibrational bond from higher to lower wave number is ascribed to the increase in the bond length of B-O groups [21].

Indeed, formation of Pb-O-B bond leads to shift of B-O band to lower wave number [24]. Similarly, incorporation of Pb into Te glasses was found to strongly shift the shoulder at 770 cm^{-1} towards 730 cm^{-1} which was attributed to the higher polarizability of Pb-O-Te linkage than Te-O-Te [25]. According to Krogh Moe's model [26] the structure of boron oxide glass consists of a random network of planar BO_3 triangles with a certain fraction of the six membered (boroxol) ring [26, 27]. In glass structure Pb^{2+} cations play the role of network modifier when these cations are ionically bonded. On the other hand, if Pb-O bond is covalent, Pb^{2+} cation will act as glass former. Because the dual role of lead ions may disrupt the glass network and form BO_4 tetrahedral units. The addition of Sm_2O_3 in increasing amounts (0.5 – 4gm) appears to suppress the effect of PbO whereby a progressive shift of BO_4 and BO_3 bands toward higher wave number is noted (Figs. 4,6). Usually, a shift of absorption bands to higher wave numbers occurs as a result of an increase in the degree of polymerization of structural network units of glass system [20]. This is accompanied by a progressive increase in the band at 465 cm^{-1} showing its maximum appearance in the spectrum of sample having 4.0gm of Sm_2O_3. This band is due to Pb-O stretching of PbO (Litharge) [28]. The effect is also the appearance of the small band at 420 cm^{-1} due to Al-O pairs. The freeing of PbO and probably Al-O from involvement in glass network is the reason for increasing the hygroscopic nature of the resulting glass matrix as inferred from the clear appearance of bands due to H-bonded water (3445, 1644 cm^{-1}), and also the bands due to OH groups (3730 cm^{-1}). Thus, up to 2 % the Sm_2O_3 acts as glass modifier.

Increasing the content of Sm_2O_3 to 2.0gm, the spectrum shows the band due to BO_4 shifted to higher frequency while composed of two maxima at 951 and 1035 cm^{-1}. The appearance of the latter band more defined compared to the case of sample "1", meanwhile of intensity comparable to that at lower wave number implies that at this level of Sm_2O_3 the BO_4 groups comprise B-O bonds of different lengths. The band due to BO_3 groups show relatively narrower profile than sample "1" with apparent increased intensity based on the comparison with the intensity of the bands due to BO_4. It can be concluded that Sm_2O_3 at 4.0gm content acts as glass modifier and former. This may find support through inspecting the region 400 – 500 cm^{-1} that shows the bands due to Pb-O and Al-O barely visible.

It can be suggested that addition of Sm_2O_3 content of $\geq$ 3.0 gm both glass formation and modification processes are taking place. It has been reported that in Sm_2O_3- B_2O_3-SiO_2- Al_2O_3 glass, Sm^{3+} exists as a network modifier. The higher Sm^{3+} concentration was, the more units of BO_3 transformed to BO_4. Nevertheless, with the increase of Sm^{3+} ions, the distances between rare earth ions would be shortened, and the dipole-quadrupole interactions would be enhanced between Sm^{3+} ions which resulted in Sm^{3+} concentration quenching. The optimum Sm^{3+} concentration was about 1 mole % [29].

This may explain the change observed in the behavior of added Sm_2O_3 i.e. concentration quenching. In the present case it seems that this has been occurred starting with $\geq$ 3.0 gm Sm_2O_3.

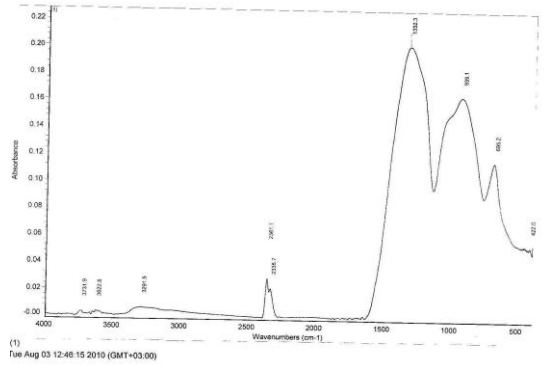

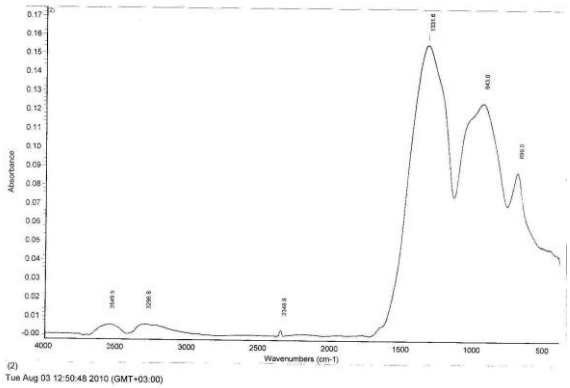

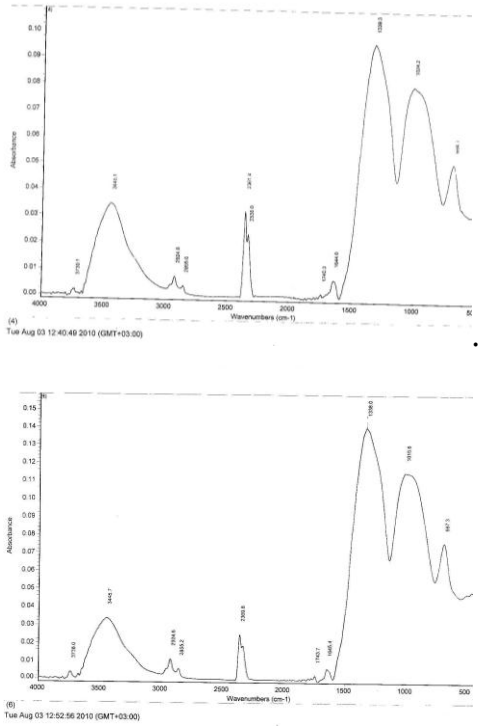

6. Conclusions

1. The correlated Pb-O and Pb-Pb pairs are evidenced in both SRO and MRO ranges in the investigated samples and arranged in the form of triangles and tetrahedral units.
2. The introduction of Sm_2O_3 with small weights in the given amorphous matrix can highly modify the structure of the MRO region. The AlO_4 pairs can be changed to AlO_6 pairs and also BO_3 pairs could be changed to BO_4 units.
3. Also, the introduced Sm_2O_3 in the studied glasses will highly distort the correlated pairs due to the formation of dangling bonds; Sm-…, separate ions of Sm^{3+} and increased bonded oxygen's to the other pairs of B-O and Al-O.
4. The formation of Sm^{2+} ions beside Sm^{3+} ones in these samples can not be evidenced in the exact ratio and Sm-O correlations are arranged in the SmO_3 units in the MRO region.
5. The addition of Sm_2O_3 with an increased ratio to the investigated amorphous matrix was found to relax the correlated linkages of Pb-Ô-Pb and Pb-Ô-B in the SRO region.
6. The IR measured for these samples give a good support to the RDF extracted information's and good agreement. The IR studies did not evidence the presence of Pb-Pb metallic pairs and also the Sm-Sm correlated MRO pairs.
7. The IR investigation evidenced well the presence of Al-O, Pb-O and both of BO_3 and BO_4 correlated pairs.

Acknowledgement

The authors wish to express their sincere gratitude to Prof. / G. El-Shafei, Chemistry Department, Faculty of Science, Ain Shams University for his helpful efforts in interpreting the data of IR for the studied samples and his fruitful discussions.

References

[1] K. Arai, H. Namikawa, K. Kumata, T. Honda, Y. Ishii, T. Handa, J. Appl. Phys. **59**, 3430 (1986).
[2] M. Nogami, T. Hagiwara, Go Kawamura, Ghaith El-Sayed, T. Hayakawa, J. Luminescence **124**, 291 (2007).
[3] A. G. Souza Filho, Filho J. Mendes, F. E. A. Melo, M. C. C. Custodio, R. Lebullenger, A. C. Hernandes, J. Phys. and Chem. of Solids **61**, 1535 (2000).
[4] E. Malchukova, B. Boizot, G. Petite, D. Ghaleb, J. Non-Crystalline Solids **353**, 2397 (2007).
[5] M. J. Weber, J. Non-Crystalline Solids **42**, 189(1980).
[6] C. Spielmann, F. Krausz, T. Brabec, E. Winter, A. Shmidt, J. Quantum Electr. **27**, 1207 (1991).
[7] M. Oomen, Adv. Mater. **3**, 403 (1991).
[8] Y. Dwivedi, A. Bahadur, S. B. Rai, J. Non-Crystalline Solids **356**, 1650 (2010).
[9] E. Malchukova, B. Boizot, D. Ghaleb, G. Petite, Nuclear Instruments and Methods in Physics Research **A537**, 411 (2005).
[10] R. Jaaniso, H. Bill, Europhys. Lett. **16**, 569 (1991).
[11] C. J. Wei, K. Holliday, A. J. Meixner, M. Croci, U. P. Wild, J. Luminescence **50**, 89 (1991).
[12] M. Nogami, T. Hiraga, T. Hayakawa, J. of Non-Crystalline Solids **241**, 98 (1998).
[13] A. Osvet, S. Emelianova, R. Weissmann, V. I. Arbuzov, A. Winnacker, J. Luminescence **86**, 323 (2000).
[14] A. C. Wright, C. A. Yarker, P. A. V. Johnson, R. N. Sinclair, J. Non-Cryst. Solids **104**, 323 (1988).
[15] J. Krogh-Moe, Acta Cryst. **9**, 951 (1956).
[16] N. Norman, Acta Cryst. **10**, 370 (1957).
[17] N. Umesaki, Y. Kita, T. Iida, K. Handa, S. Kohara, K. Suzuya, T. Fukunaga, M. Misawa, Phys. and Chem. Glasses **41**(5), 304 (2000).
[18] R. M. Abdelouhab, R. Braunstein, K. Barner, J. Non-Crystalline Solids **108**, 109 (1989).
[19] S. G. Motke, S. P. Yawake, S. S. Yawake, Bull. Mater. Sci. **25**(1), 75 (2002).
[20] G. Upender, C. P. Vardhani, V. Kamalaker, V. Chandra, Mouli, SRX Physics 2010, 1-6-doi: 10.3814/2010/927056 (2010).
[21] Virender Kundu, R. I. Dbiman, A. S. Maan, D. R. Goyal, Advances in Condensed Matter Physics (2008).
[22] I. Andelean, Simon Cora, V. Ioncu, J. Optoelectron. Adv. Mater. **8**(5), 1843 (2006).
[23] S. G. Motke, S. P. Yawake, S. S. Yawale, Bull. Mater. Sci. **25**(1), 75 (2002).
[24] S. G. Motke, S. P. Yawake, S. S. Yawale, J. Non-Cryst. Solids **324**, 12 (2003).
[25] D. Munoz-Martis, M. A. Villegas, J. Gonzala, J. M. Fernandez-Navarro, J. Eur. Ceram. Soci. **29**(14), 2903 (2009).
[26] J. Krogh Moe, J. Phys. Chem. Glasses **6**,4 6 (1965).
[27] J. Krogh Moe, J. Non-Cryst. Solids **1**, 269 (1969).
[28] William B. White, Rustum Roy, Amer. Miner. **49**, 1670 (1964).
[29] Yaru Ni, Chunhua Lu, Zhang Yan, Zhang Qitu, Zhngzi Xu. J. Rare Earths **25**, 94 (2007).

*Corresponding author: aliaboshama_1@hotmail.com